Characterizing a global aviation radiation environment baseline with models and measurement databases

W Kent Tobiska[1], Christopher Mertens[2], and Yihua Zheng[3]

[1]Space Environment Technologies
[2]NASA Langley Research Ctr
[3]NASA/GSFC

November 23, 2022

Abstract

Two major sources of radiation hazards at commercial aviation altitudes have been known for decades and those are galactic cosmic rays (GCRs) as well as solar energetic particles (SEPs). GCRs are produced outside the solar system in high-energy explosive events and consist mostly of energetic protons slowly modulated by the strength of the Sun's interplanetary magnetic field (IMF). SEPs come from either solar coronal mass ejections (CMEs) related to flaring events or from IMF shocks. In the latter case fast CMEs plow through a slower solar wind creating a shock front to produce energetic protons. Recently, a third radiation source has been identified that originates from relativistic electron precipitation (REP) associated with the Van Allen radiation belts and have been called radiation clouds although a physical perspective is likely to be flight through a γ-ray beam. This ensemble radiation field creates safety concerns for aviation. Because of this safety hazard, a broad community is seeking to i)define the requirements for real-time monitoring of the charged particle radiation environment to protect the health and safety of crew and passengers during space weather events; ii)define the scope and requirements for a real-time reporting system that conveys situational awareness of the radiation environment to orbital, suborbital, and commercial aviation users during space weather events; and iii)develop or improve models for the real-time assessment of radiation levels at commercial flight altitudes. While benchmarks for ionizing radiation related to aviation have included characterizing an occurrence frequency of 1 in 100 years and an intensity level at the theoretical maximum for radiation events, it is also important to develop a baseline radiation environment for GCRs, SEPs, and REPs against which events can be compared. We describe functional, analytical baselines for describing the ionizing radiation environment for commercial aviation based on observations and modeling as part of the NAIRAS, ARMAS, and RADIAN programs.

SPACE ENVIRONMENT TECHNOLOGIES
Space Weather Division

Characterizing a global aviation radiation environment baseline with models and measurement databases

SM31C-1795-3511

W Kent Tobiska, Brad Gersey, Chris Mertens, Yihua Zheng and the ARMAS Science Team

ABSTRACT & PROGRESS

ABSTRACT. Two major sources of radiation hazards at commercial aviation altitudes have been known for decades and those are galactic cosmic rays (GCRs) as well as solar energetic particles (SEPs). GCRs are produced outside the solar system in high-energy explosive events and consist mostly of energetic protons slowly modulated by the strength of the Sun's interplanetary magnetic field (IMF). SEPs come from either solar coronal mass ejections (CMEs) related to flaring events or from IMF shocks. In the latter case fast CMEs plow through a slower solar wind creating a shock front to produce energetic protons. Recently, a third radiation source has been identified that originates from relativistic electron precipitation (REP) associated with the Van Allen radiation belts and have been called radiation clouds although a physical perspective is likely to be flight through a γ-ray beam. This ensemble radiation field creates safety concerns for aviation. Because of this safety hazard, a broad community is seeking to *i)* define the requirements for real-time monitoring of the charged particle radiation environment to protect the health and safety of crew and passengers during space weather events; *ii)* define the scope and requirements for a real-time reporting system that conveys situational awareness of the radiation environment to orbital, suborbital, and commercial aviation users during space weather events; and *iii)* develop or improve models for the real-time assessment of radiation levels at commercial flight altitudes. While benchmarks for ionizing radiation related to aviation have included characterizing an occurrence frequency of 1 in 100 years and an intensity level at the theoretical maximum for radiation events, it is also important to develop a baseline radiation environment for GCRs, SEPs, and REPs against which events can be compared. We describe functional, analytical baselines for describing the ionizing radiation environment for commercial aviation based on observations and modeling as part of the NAIRAS, ARMAS, and RADIAN programs.

GCR, SEP and EEP radiation environment

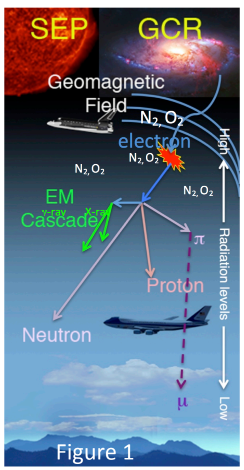

(Left panel – Figure 1) The radiation environment at commercial aviation altitudes.

(Right panel, upper – Figure 2) Global ARMAS for 594 flights with 522050 one-minute data records. Data at altitudes ≥8 km. Also shown is primary proton environment above 20 km organized by cutoff rigidities, Rc.

(Right panel, lower– Figure 3) High magnetic latitudes showing excess REP radiation in auroral zone.

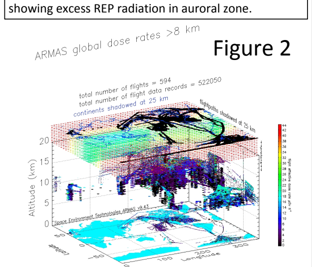

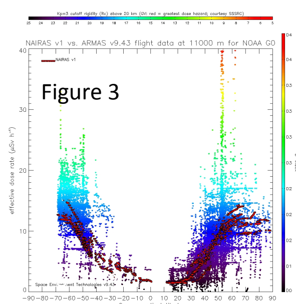

ARMAS AND RADIAN PROGRESS TO DATE:

Three relevant radiation sources recognized

1. GCRs – ubiquitous and isotopic around the planet; modulated by solar cycle
2. SEPs – rare and directed in the polar cap regions; event driven by CMEs and IMF shocks (NOT OBSERVED)
3. **REPs – ubiquitous and directed in auroral zones (2<L<7); frequent precipitation even during quiet geomagnetic conditions (G0)**

Measurements accomplished

1. **Greater than ½ million one-minute data records**
2. **Altitude range from surface to 50 km**
3. **Magnetic latitudes +80 to -80 degrees and all longitudes**
4. **Solar cycle 24 maximum (2013) to minimum (2018)**
5. No SEPs or large geomagnetic storms observed (>G2)

Instrument flight and model comparisons accomplished

1. **ARMAS FM5 and TEPC flown together across CONUS**
2. **ARMAS and NAIRAS baselines compared (see SWJ article)**
3. **12 ARMAS instruments now span 6 generations**

POSSIBLE HEALTH IMPLICATIONS: 3 dose types (tissue) recognized

1. Deep tissue – heavy ions above 30 km (commercial space)
2. Deep tissue – protons and neutrons (commercial air)
3. **Surface tissue – gamma-rays and X-rays (commercial air)**
4. **Crew and passengers can get 10-25% more dose on North Atlantic and North Pacific routes than expected from GCRs.**

http://sol.spacenvironment.net/~ARMAS/index.html

GCR Analytical Representation

Publication details of study: Tobiska, W.K., L. Didkovsky, K. Judge, S. Wieman, D. Bouwer, J. Bailey, B. Atwell, M. Maskrey, C. Mertens, Y. Zheng, M. Shea, D. Smart, B. Gersey, R. Wilkins, D. Bell, L. Gardner, and R. Fuschino (2018), Analytical Representations for Characterizing the Global Aviation Radiation Environment based on Model and Measurement Databases, Space Weather, 16, (10), 1523–1538. **Available as Open Access at https://agupubs.onlinelibrary.wiley.com/doi/10.1029/2018SW001843**

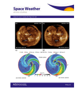

We have developed a set of analytical function coefficients that, when used in equation (1), represent NAIRAS climatological and ARMAS median statistical weather databases shown in Figures 4 and 5. Equation (1) generates the effective dose rate, *dE/dt*, in μSv h^{-1} as a function of the McIlwain L-shell (between 1.5 ≤ L ≤ 10), the NOAA G-scale geomagnetic conditions (between G0 and G3), and altitude (between 9 and 14 km). Equation (1) represents only the GCR component of the aviation radiation environment and excludes contributions from either SEPs or REPs. It is a 9th degree polynomial fit to the databases and is given as:

$$dE/dt\,(L)_{z,GX} = A_0 + A_1L + A_2L^2 + A_3L^3 + A_4L^4 + A_5L^5 + A_6L^6 + A_7L^7 + A_8L^8 + A_9L^9 \qquad \mu Sv\ h^{-1} \qquad (1)$$

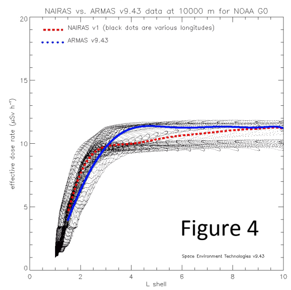

(Figure 4) Median ARMAS (blue) and NAIRAS (red) GCR effective dose rates by L-shell, NOAA G0, and 10 km altitude.

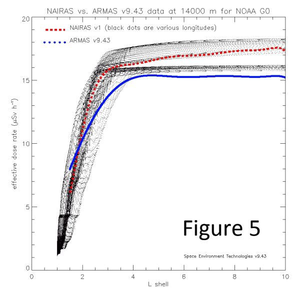

(Figure 5) Median ARMAS (blue) and NAIRAS (red) GCR effective dose rates by L-shell, NOAA G0, and 14 km altitude.

REP Analytical Representation

While the ARMAS database is still sparse in several domains, we are able to recommend a subset of eight cases that represent the GCR + REP combined median value for NOAA G0 and G1 geomagnetic conditions and altitudes of 9, 10, 11, 12 and 13 km for 1.5 ≤ L ≤ 5. In Figures 6 and 7 we show effective dose rate vs. L-shell at a constant 11 and 12 km altitudes and G0 geomagnetic conditions. There were no SEP radiation sources during these flights. The heavy black and red lines through the ARMAS data are the mean and median polynomial fits, respectively, that show the effect of REPs combined with the slowly varying GCR background radiation component during 2013 – 2018, i.e., from solar cycle 24 decline to minimum. The black dotted line is the GCR background alone for ARMAS. The polynomial fit to the median GCR *plus* REP data yields equation (2) for an enhanced effective dose rate, *dE/dt*, (μSv h^{-1}). The median value coefficients for eight cases are a 2nd degree polynomial fit:

$$dE/dt\,(L)_{z,GX} = B_0 + B_1L + B_2L^2 \qquad \mu Sv\ h^{-1} \qquad (2)$$

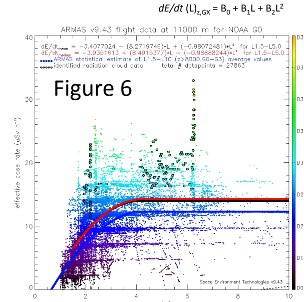

(Figure 6) ARMAS effective dose rate GCR statistical background (black dotted line), median GCR+REP database (red), and mean GCR+REP database (black), for NOAA G0 geomagnetic conditions at 11 km (equation 2).

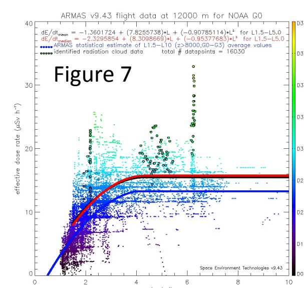

(Figure 7) ARMAS effective dose rate GCR statistical background (black dotted line), median GCR+REP database (red), and mean GCR+REP database (black), for NOAA G0 geomagnetic conditions at 12 km (equation 2).

Climatological forecasting and data assimilation

As a start toward hemispheric climatological and statistical weather forecasting, we provide examples in Figure 8 showing the northern hemisphere for geomagnetic conditions of G0, G2 and G4 at twelve altitude layers (8 – 19 km in 1 km steps for G0). This visual interpretation, which includes the D-index color scale alongside the effective dose rate, makes it very easy for pilots and air traffic management to assess near-term, future radiation safety hazards. Space Environment Technologies (SET) continuously forecasts the hourly geomagnetic conditions for Dst using two independent methods: its Anemomilos algorithm (Tobiska *et al.*, 2013) and the NOAA Space Weather Prediction Center ENLIL model plus Rice University Dst neural net algorithm. The results of these predictions from both algorithms are available at the URL https://sol.spacenvironment.net/~sam_ops/index.html?. Separately, the hourly Dst is transformed into a NOAA G-scale value in the SET operational system and becomes the basis for creating the climatology forecast of the GCR radiation environment shown in Figures 4, 5 and 8. Current operational forecasting is done for 1-hour time granularity out to 144 hours (6 days) in the future. Very near term (a few hours) forecasts are more accurate than longer-term (days) forecasts. SET is updating its operations for producing statistical weather forecasts of the GCR+REP environment in the 2 < L < 7 REP precipitation bands.

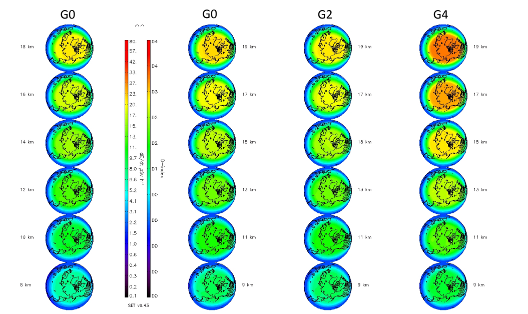

(Figure 8) Climatological NAIRAS effective dose rates from GCRs showing the northern hemisphere for geomagnetic conditions of G0, G2 and G4 at twelve altitude layers (8 – 19 km in 1 km steps for G0). This visual interpretation includes the D-index color scale alongside the effective dose rate.

Regions, airports, and routes. Examples of how forecasts might be applied to regions, airports, and individual aircraft routes are shown in Figures 9 and 10. Both the dE/dt effective dose rate and the D-index are shown in these examples for a commercial aircraft at 11 km on 10 April 2016 flying from Los Angeles to Washington DC under G0 (quiet) geomagnetic conditions. The effective dose rate measured on the aircraft was slightly less than the forecast values for that flight for much of the flight. An advantage of this type of forecast data product is that regional air traffic management centers, local international airports, and aircraft operations can all benefit from forecast products using the baseline GCR rates. We are beginning to use the ARMAS data for assimilation into NAIRAS to obtain the weather of the radiation environment.

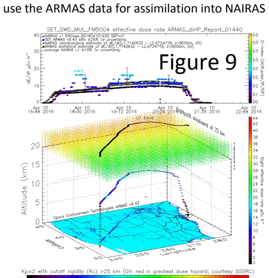

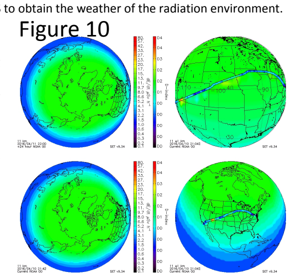

(Figure 9) effective dose rate vs. time for the LA-DC flight (top panel); regional flight track of a LA–DC flight (bottom right).

(Figure 10) 24 h northern hemisphere forecast (top left); the current epoch (bottom left); the regional flight track of a LA–DC flight (top right); and the hemispheric view of the LA–DC flight (bottom right).